OPEN ACCESS
IOP Publishing
Plasma Physics and Controlled Fusion
Plasma Phys. Control. Fusion **66** (2024) 025011 (5pp)
https://doi.org/10.1088/1361-6587/ad1ae3

The radial localization of the transition from low to high confinement mode in the ASDEX Upgrade tokamak

M Cavedon[1,2,*], T Happel[2], P Hennequin[3], R Dux[2], K Höfler[4], U Plank[2], T Pütterich[2], U Stroth[2], E Viezzer[5], E Wolfrum[2] and the ASDEX Upgrade Team[2]

[1] Department of Physics 'G. Occhialini', University of Milan-Bicocca, Milan, Italy
[2] Max Planck Institute for Plasma Physics, Garching, Germany
[3] Laboratoire de Physique des Plasmas, CNRS, Sorbonne Université, École polytechnique, Institut Polytechnique de Paris, Palaiseau, France
[4] Max Planck Institute for Plasma Physics, Greifswald, Germany
[5] Department of Atomic, Molecular and Nuclear Physics, University of Seville, Seville, Spain

E-mail: marco.cavedon@unimib.it

Received 13 July 2023, revised 28 November 2023
Accepted for publication 4 January 2024
Published 11 January 2024

Abstract

A novel experimental method is applied to localize the initial suppression of turbulence, in the form of density fluctuations, at the transition from the low (L-) to the high (H-) confinement mode in toroidal magnetic fusion plasmas. The high radial and temporal resolution, combined with the unprecedented statistical significance, provided the awaited information on a possible dominant $\mathbf{E} \times \mathbf{B}$ shear layer in L-H transition physics. We show, for the first time, that the H-mode turbulence suppression is initiated at the inner $\mathbf{E} \times \mathbf{B}$ shear layer in the ASDEX Upgrade tokamak possibly shedding light on the causality behind the L-H transition process.

Keywords: L-H transition, $\mathbf{E} \times \mathbf{B}$ shear, shear layer

1. Introduction

The physics of the L-H transition in toroidal magnetically confined plasmas is a persisting enigma which has a critical implication for achieving efficient energy production in a fusion reactor that is to be operated in H-mode. The leading explanation for the L-H transition and the amount of heating power P_{thr} required to access it is the $\mathbf{E} \times \mathbf{B}$ shear stabilization of turbulence at the plasma edge [1]. The $\mathbf{E} \times \mathbf{B}$ velocity ($v_{E\times B} = E_r/B$) in the confined region may result from any non-ambipolar transport mechanism, e.g. ion orbit losses [2], collisional (neoclassical) processes [3], or from turbulence stresses [4]. Here, E_r is the radial electric field and B is the magnetic field strength. Outside the last closed flux surface (or separatrix), in the so-called Scrape-Off Layer (SOL), E_r is mostly determined by the non-ambipolar parallel transport of ions and electrons defining the plasma potential via a sheath region in front of the targets [5]. In the confined region inside the separatrix, the $\mathbf{v}_{\mathrm{E\times B}}$ profile shape features two shear layers, hereafter referred to as the inner and outer layers. The knowledge of which shear layer is responsible for the L-H transition is crucial to tailor experimental strategies aimed to influence the dominant shear layer and, in turn, optimize the H-mode access. Several previous works have already shown the impact of the $\mathbf{E} \times \mathbf{B}$ flow shear on turbulence [6–9]. In this Letter, we show, thanks to state-of-the-art diagnostics and advanced analysis, the possibility to identify at which shear layer the turbulence is firstly stabilized at the L-H transition.

In recent years, several experimental and modeling results pointed to the influence of the SOL and divertor conditions on

* Author to whom any correspondence should be addressed.

the L-H power threshold. At the JET tokamak, it was observed that $P_{\rm thr}$ increases with the X-point height and decreases with the divertor closure [10]. Similar observations were obtained at the DIII-D and MAST tokamaks [11, 12]. Along the same lines, modeling results showed a correlation between $P_{\rm thr}$ and $\mathbf{v}_{\rm E\times B}$ just outside the last closed flux surface which could point to the importance of the nearby outer shear layer in the L-H transition physics [13]. Moreover, in an interchange-drift-Alfvén turbulence model, the separatrix parameters well sort out the ASDEX Upgrade confinement [14]. However, the model describes the H-mode sustainment but not its triggering. Finally, a theory based on the relative alignment of the $\mathbf{E}\times\mathbf{B}$ shear and the Reynold stress predicts a positive coupling to the outer shear due to the symmetry breaking of the magnetic shear at the X-point [15]. All of these findings would suggest a dominant role of the outer shear layer. On the other hand, a correlation between the edge ion heat flux and the H-mode onset has been found in ASDEX Upgrade and ALCATOR C-mod [16, 17] suggesting that the inner shear layer is the relevant one for the L-H transition. Finally, zonal flows can impact both the outer and the inner layer [18–20]. These are, however, all indirect and not conclusive indications since outer and inner shear layers are strongly coupled. For instance, an increase of the $\mathbf{E}\times\mathbf{B}$ velocity at the inner shear would at the same time steepen the outer one while a change in the divertor conditions might also affect the density and temperature gradients within the separatrix and, in turn, the inner $\mathbf{E}\times\mathbf{B}$ shear. For these reasons, it is essential to directly measure the impact of the shear layer on the turbulence in the edge region. If the impact can be pinpointed temporally and locally, the shear region that plays the key role can be identified. The knowledge of the dominant shear layer for the L-H transition physics might help in validating any model of it.

2. Experiments

We present a novel method to radially localize the initial suppression of density fluctuations at the L-H transition. It exploits the Doppler reflectometry (DR) diagnostic, allowing to probe both the density fluctuation amplitude (in a limited wavenumber range), and the fluctuation propagation velocity, with a sub-μs time resolution and spatial sensitivity at the mm scale. Density fluctuations are a marker of the local turbulence and their reduction at the L-H transition has been a well-recognized and fundamental characteristic of this transition almost since its discovery [21]. Furthermore, density fluctuations are frequently employed as indicators of the overall turbulence behavior, particularly when investigating the interplay between turbulence and flows as the L-H transition [9, 18]. Therefore, in the following, we will at times use the term 'turbulence' and 'density fluctuations' interchangeably.

The key of the method is the development of a discharge scenario where L-H-L dithers, typically at a frequency around 100 Hz [7, 10, 22], are present for a long time interval. To achieve this, the heating power has to be finely tuned just above

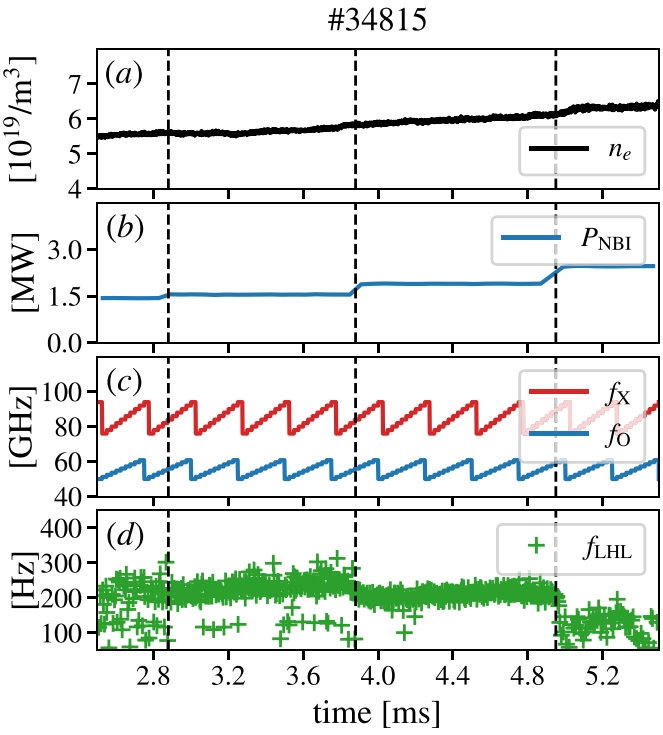

Figure 1. Repetitive L-H-L dither discharge scenario: (a) line-averaged electron density, (b) NBI power, (c) DR probing frequency of the X-mode (red) and O-mode (blue) systems, (d) L-H-L dithers frequency.

$P_{\rm thr}$, while the electron density $n_{\rm e}$ is in the range where $P_{\rm thr}$ increases with density. This assures a fall back into L-mode after the rise of the density following the L-H transition [23]. Figure 1 shows such scenario with standard lower single null edge optimized shape, favorable $B\times\nabla B$ drift, plasma current of $I_{\rm p}=0.8$ MA, $B_t=-2.5$ T, and safety factor $q_{95}=5.3$: the Neutral Beam Injection (NBI) power (figure 1(b)) is stepped by changing the NBI duty cycle, resulting in different phases, separated by the vertical lines, where the line averaged electron density (figure 1(a)) remains in the same range, while the L-H-L dithers frequency $f_{\rm LHL}$ (figure 1(d)) is changed. Within one phase, two DR systems, one in X-mode and one in O-mode, probe the plasma at frequencies scanned respectively in the range 76 GHz – 94 GHz and 50 GHz – 60.8 GHz four times (figure 1(c)). These frequencies corresponds to perpendicular wave number ranges of roughly $10\div14$ cm^{-1} for the X-mode and $7\div9$ cm^{-1} for the O-mode, which typically coincides with the transition between ion and electron modes (ITG—ETG) still below electron temperature gradient mode peak in the k-spectra [24]. Here, we only show the analysis of the time window between 3.9 s and 4.9 s in which $f_{\rm LHL}$ is mostly stable at around 200 Hz, however the same results were obtained also in the other phases. The frequency $f_{\rm LHL}$ is calculated using the poloidal magnetic field fluctuation ($\dot{B}_\theta$) signal measured by a magnetic pick-up coil close to the X-point [25, 26]. An example of few L-H-L dithers as measured by the coil are shown in figure 2(a), where the H- and the L-mode parts are shaded in gray and green, respectively. Roughly 150 out of

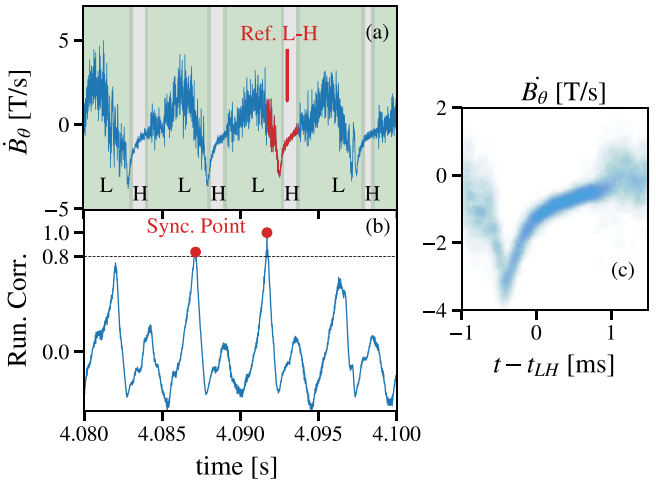

Figure 2. Synchronization procedure: (a) define a reference L-H transition (red) using the $\dot{B}_\theta$ signal; calculate the running correlation (b) and set an acceptance threshold (in this case 0.8); use the maximum of the correlation for every L-H transition (in red in (b)) as synchronization time-point. Figure (c) shows the synchronized $\dot{B}_\theta$ over 150 L-H dithers.

the total 200 L-H transitions within the reference phase have been selected and synchronized using an algorithm based on the running correlation of one reference L-H-L dither $\dot{B}_\theta$ signature with the other dithers. A threshold in the correlation of 0.8 has been used to select only similar L-H transitions and the maximum correlation for a given transition as the synchronization time point. Figure 2(a) shows the reference L-H transition and other three L-H-L dithers, in figure 2(b) the running correlation and in figure 2(c) the synchronized $\dot{B}_\theta$ over the 150 L-H transitions. The exact definition of the L-H time point t_{LH} is arbitrary and it has been defined by means of the turbulence measurement as shown later. Due to the large number of L-H transitions considered, the statistical significance of this analysis is much higher than in earlier L-H transition studies in which often only one or, in best cases, a few L-H transitions were investigated.

3. Results

Figure 3 shows the amplitude of n_{e} fluctuation level, i.e. the amplitude of the DR signal A_{DR}, for the X-mode (figure 3(a)) and the O-mode channel (figure 3(b)) synchronized to the one L-H-L dither and conditionally averaged as a function of the normalized plasma radius ρ_{pol} and time. Red indicates high turbulence level while blue shows low turbulence level. Note that A_{DR} is the measurement of the back-scattered microwave signal which can be used only as a qualitative monitor of the n_{e} fluctuation, while a quantitative estimation of $\tilde{n_{\mathrm{e}}}$ is not possible [27]. Nevertheless, in this work, we analyzed both the O-mode and X-mode systems to highlight the consistency and robustness of the results as they respond differently to the turbulence amplitude [24]. The radial positions associated with the probing frequencies have been traced during the L-H-L cycle (in figure 3, see movement in time of the location of the measurements). The mapping was done by means of a ray-tracing code [28] with the density profiles obtained by synchronizing and conditionally averaging the of the electron density from the lithium beam emission spectroscopy diagnostic [29]. The radial uncertainty in the density profile derived from the Li beam measurements is approximately 3 mm within the specified region. This uncertainty encompasses the effects of both the radial integration of the Li beam measurement channel and the finite lifetime of the Li2p excited state. The n_{e} profile temporal resolution is the result of the binning the raw data, which is originally sampled at 1 microsecond intervals, and has been set to 200 μs to obtain a relatively accurate emission profile for the reconstruction of electron density. As for the equilibrium reconstruction, it is based on a pressure-constrained equilibrium with a time resolution of 100 microseconds [30]. We do not expect significant changes on shorter time scales as these are prevented by the passive stabilizing loop structure present in AUG.

The synchronized DR data in figure 3 are binned to an equivalent temporal resolution of 10 μs which is the horizontal extension of the pixels, while the vertical one is the radial resolution from the ray-tracing code. Note that the turbulence level measured by DR for a certain frequency A_{DR} is normalized to its mean value $\langle A_{\mathrm{DR}} \rangle$ before the L-H transition ($t \in [-0.5, 0]$ ms) to emphasize relative changes and to take into account the variation of the launched microwave power with the probing frequency. Both O-mode and X-mode channels show a localized initial turbulence decrease at $\rho_{\mathrm{pol}} \approx 0.98$ at the L-H transition which extends towards the last close flux surface and the plasma center within few microseconds. To our knowledge, this is the first time that the L-H transition could be radially localized with this accuracy.

To determine at which $\mathbf{E} \times \mathbf{B}$ shear layer the initial turbulence reduction is triggered, the $\mathbf{E} \times \mathbf{B}$ velocity right before the transition needs to be determined. This can be done directly from the DR data. Thus uncertainties in the equilibrium reconstruction and in the relative alignment of different diagnostics are avoided. In principle, to localize the initial turbulence relative to the $\mathbf{v}_{\mathrm{E\times B}}$ shear layers, it is not necessary to map the DR signals on ρ_{pol} since we could just look at the probing frequencies. This is of crucial importance because we want to detect a phenomenon on the 1mm scale and the usual uncertainties of the equilibrium reconstruction are in the range of millimeters. The measurements are nevertheless shown mapped to help the reader understand the analysis method. Figure 4 shows the $\mathbf{v}_{\mathrm{E\times B}}$ profiles from the X-mode (red) and O-mode (blue) channels, evaluated within the last 0.5 ms before the L-H transition. The $\mathbf{v}_{\mathrm{E\times B}}$ minimum is roughly consistent with previous studies using the DR diagnostic [31]. The absolute values are lower than the CXRS measurements in [32] while the position and the values of the gradients are compatible. The position of the initial turbulence suppression, i.e. $\rho_{\mathrm{pol,shear}} \approx 0.98$ (see figure 3), is indicated by the black vertical line and it is clearly located within the inner shear layer for both X- and O-mode.

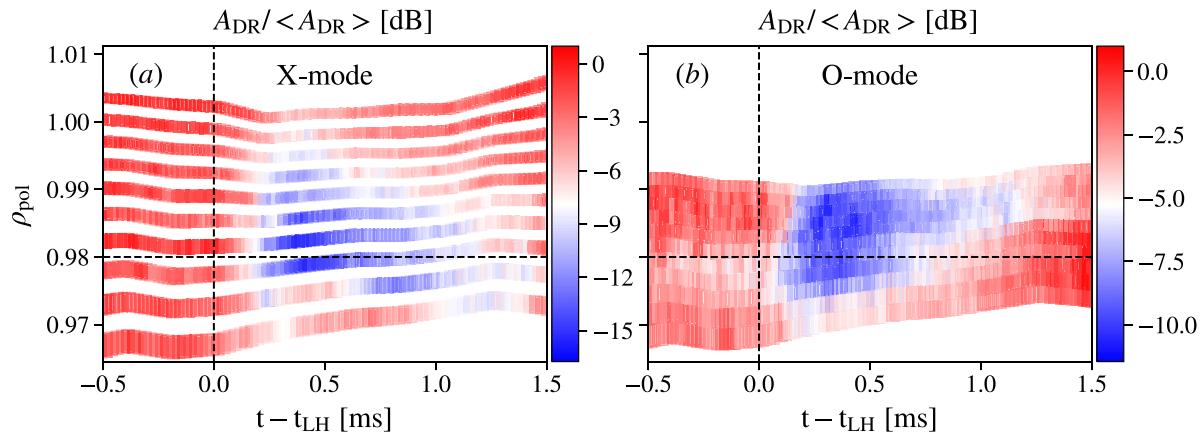

Figure 3. Synchronized turbulence level A_{DR} normalized to the pre-L-H during an L-H-L transition from (a) X-mode DR and (b) O-mode DR. High to low turbulence levels are color coded from red to blue. The dashed horizontal line indicate roughly the initial turbulence suppression position and the vertical line the L-H transition time point.

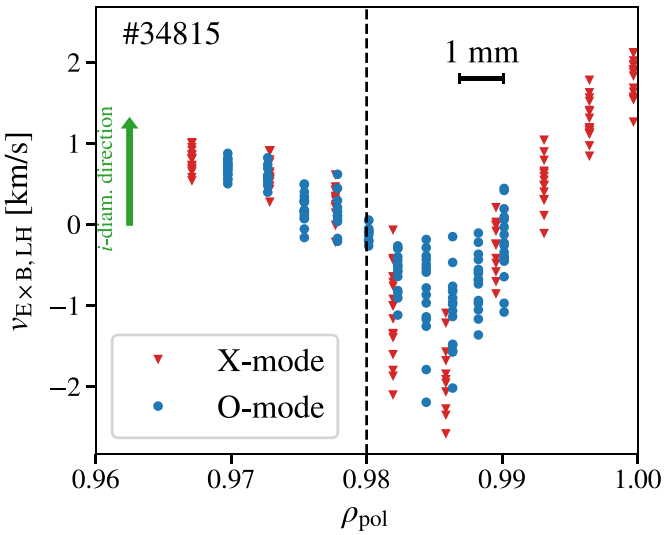

Figure 4. Synchronized $\mathbf{v}_{E\times B}$ profiles over 150 L-H dithers, right before the L-H transition ($t - t_{LH} \in [-0.5, 0.0]$ ms): X-mode DR (red) and O-mode DR (blue). The vertical line indicates the radial position of the initial turbulence suppression.

4. Conclusion and outlook

To conclude, we developed a new method to localize the L-H transition based on DR and on a plasma scenario with repetitive L-H-L dithers. The high statistical significance, combined with the high temporal and radial resolution allowed us to answer the long-standing question on a possible dominant shear layer in the L-H transition. In this Letter, we provide the evidence that the turbulence, in the form of density fluctuations, suppression at the L-H transition is initiated at inner $\mathbf{E} \times \mathbf{B}$ shear layer. Efforts in modeling and understanding the L-H transition shall therefore focus on the behavior of the inner $\mathbf{E} \times \mathbf{B}$ shear, or more in general, in reproducing this feature of the L-H transition phenomenology. Finally, the simplicity of the method to localize the L-H transition proposed in this Letter makes it well applicable to any fusion plasma device equipped with DR, allowing a direct comparison to the results shown here.

As an outlook, the newly installed Comb-Reflectometry at ASDEX Upgrade will offer the possibility to measure simultaneously at several different sampling frequencies providing time resolved A_{DR} profiles without the need of repetitive L-H transitions [33]. This will open the possibility to investigate many different scenarios and to test single step transitions against repetitive L-H-L dithers.

Data availability statement

The data cannot be made publicly available upon publication because no suitable repository exists for hosting data in this field of study. The data that support the findings of this study are available upon reasonable request from the authors.

Acknowledgments

The authors would like to thank P Manz, G Harrer and O Grover for their valuable and constructive suggestions during the development of this research work.

ORCID iDs

M Cavedon https://orcid.org/0000-0002-0013-9753
T Happel https://orcid.org/0000-0003-4364-9363
P Hennequin https://orcid.org/0000-0002-4848-4898
K Höfler https://orcid.org/0000-0001-7925-8159
U Plank https://orcid.org/0000-0002-1509-4308
T Pütterich https://orcid.org/0000-0002-8487-4973
U Stroth https://orcid.org/0000-0003-1104-2233
E Viezzer https://orcid.org/0000-0001-6419-6848
E Wolfrum https://orcid.org/0000-0002-6645-6882

References

[1] Biglari H, Diamond P H and Terry P W 1990 Influence of sheared poloidal rotation on edge turbulence *Phys. Fluids* B **2** 1

[2] Shaing K C and Crume E C 1989 Bifurcation theory of poloidal rotation in tokamaks: a model for L-H transition *Phys. Rev. Lett.* **63** 2369–72

[3] Hinton F L and Hazeltine R D 1976 Theory of plasma transport in toroidal confinement systems *Rev. Mod. Phys.* **48** 239–308

[4] Diamond P H, Itoh S I, Itoh K and Hahm T S 2005 Zonal flows in plasma – a review *Plasma Phys. Control. Fusion* **47** R35

[5] Stangeby P and Chankin A 1996 Simple models for the radial and poloidal E × B drifts in the scrape-off layer of a divertor tokamak: effects on in/out asymmetries *Nucl. Fusion* **36** 839–52

[6] Tynan G R, Schmitz L, Conn R W, Doerner R and Lehmer R 1992 Steady-state convection and fluctuation-driven particle transport in the H-mode transition *Phys. Rev. Lett.* **68** 3032–5

[7] Burrell K H 1999 Tests of causality: experimental evidence that sheared E × B flow alters turbulence and transport in tokamaks *Phys. Plasmas* **6** 4418–35

[8] Estrada T, Hidalgo C, Happel T and Diamond P H 2011 Spatiotemporal structure of the interaction between turbulence and flows at the L-H transition in a toroidal plasma *Phys. Rev. Lett.* **107** 245004

[9] Conway G D, Angioni C, Ryter F, Sauter P and Vicente J 2011 Mean and oscillating plasma flows and turbulence interactions across the L-H confinement transition *Phys. Rev. Lett.* **106** 065001

[10] Delabie E *et al* 2014 Overview and interpretation of L-H Threshold Experiments on JET with the ITER-like Wall *EX/P5-24, 25th IAEA Fusion Energy Conf.* (*Saint Petersburg, Russia*)

[11] Gohil P, Evans T, Fenstermacher M, Ferron J, Osborne T, Park J, Schmitz O, Scoville J and Unterberg E 2011 L–H transition studies on DIII-D to determine H-mode access for operational scenarios in ITER *Nucl. Fusion* **51** 103020

[12] Meyer H *et al* 2011 L–H transition and pedestal studies on MAST *Nucl. Fusion* **51** 113011

[13] Chankin A *et al* 2017 Possible influence of near sol plasma on the H-mode power threshold *Nucl. Mater. Energy* **12** 273–7

[14] Eich T and Manz P the ASDEX Upgrade team 2021 The separatrix operational space of ASDEX upgrade due to interchange-drift-Alfvén turbulence *Nucl. Fusion* **61** 086017

[15] Fedorczak N, Ghendrih P, Hennequin P, Tynan G R, Diamond P H and Manz P 2013 Dynamics of tilted eddies in a transversal flow at the edge of tokamak plasmas and the consequences for L–H transition *Plasma Phys. Control. Fusion* **55** 124024

[16] Ryter F, Barrera Orte L, Kurzan B, McDermott R, Tardini G, Viezzer E, Bernert M and Fischer R 2014 Experimental evidence for the key role of the ion heat channel in the physics of the L–H transition *Nucl. Fusion* **54** 083003

[17] Schmidtmayr M *et al* 2018 Investigation of the critical edge ion heat flux for L-H transitions in Alcator C-Mod and its dependence on B_T *Nucl. Fusion* **58** 056003

[18] Schmitz L, Zeng L, Rhodes T L, Hillesheim J C, Doyle E J, Groebner R J, Peebles W A, Burrell K H and Wang G 2012 Role of zonal flow predator-prey oscillations in triggering the transition to H-mode confinement *Phys. Rev. Lett.* **108** 155002

[19] Xu G S *et al* 2016 Low-to-high confinement transition mediated by turbulence radial wave number spectral shift in a fusion plasma *Phys. Rev. Lett.* **116** 095002

[20] Hillesheim J C, Delabie E, Meyer H, Maggi C F, Meneses L and Poli E (JET Contributors, EUROfusion Consortium, JET, Culham Science Centre, Abingdon, Oxon OX14 3DB, United Kingdom Contributors fusion Consortium, JET, Culham Science Centre, Abingdon, Oxon OX14 3DB, United Kingdom) 2016 Stationary zonal flows during the formation of the edge transport barrier in the JET tokamak *Phys. Rev. Lett.* **116** 065002

[21] Matsumoto H *et al* 1992 Suppression of the edge turbulence at the L-H transition in DIII-D *Plasma Phys. Control. Fusion* **34** 615

[22] Cavedon M, Pütterich T, Viezzer E, Birkenmeier G, Happel T, Laggner F M, Manz P, Ryter F and Stroth U (the ASDEX Upgrade Team) 2017 Interplay between turbulence, neoclassical and zonal flows during the transition from low to high confinement mode at ASDEX upgrade *Nucl. Fusion* **57** 014002

[23] Ryter F *et al* (the ASDEX Upgrade Team) 2013 Survey of the H-mode power threshold and transition physics studies in ASDEX upgrade *Nucl. Fusion* **53** 113003

[24] Happel T *et al* 2017 Comparison of detailed experimental wavenumber spectra with gyrokinetic simulation aided by two-dimensional full-wave simulations *Plasma Phys. Control. Fusion* **59** 054009

[25] Solano E R 2016 Axisymmetric oscillations at L–H transitions in JET: M-Mode *Nucl. Fusion* **57** 022021

[26] Birkenmeier G *et al* 2016 Magnetic structure and frequency scaling of limit-cycle oscillations close to L- to H-mode transitions *Nucl. Fusion* **56** 086009

[27] Hirsch M, Holzhauer E, Baldzuhn J, Kurzan B and Scott B 2001 Doppler reflectometry for the investigation of propagating density perturbations *Plasma Phys. Control. Fusion* **43** 1641

[28] Poli E, Peeters A and Torbeam P G 2001 A beam tracing code for electron-cyclotron waves in tokamak plasmas *Comput. Phys. Commun.* **136** 90–104

[29] Willensdorfer M, Wolfrum E, Fischer R, Schweinzer J, Sertoli M, Sieglin B, Veres G and Aumayr F 2012 Improved chopping of a lithium beam for plasma edge diagnostic at ASDEX upgrade *Rev. Sci. Instrum.* **83** 023501

[30] Fischer R *et al* 2013 Magnetic equilibrium reconstruction using geometric information from temperature measurements at ASDEX upgrade *Proc. 40th EPS Conf Plasma Phys.*

[31] Plank U *et al* 2023 Experimental study of the edge radial electric field in different drift configurations and its role in the access to H-mode at ASDEX Upgrade *Phys. Plasmas* **30** 042513

[32] Cavedon M *et al* 2020 Connecting the global h-mode power threshold to the local radial electric field at ASDEX upgrade *Nucl. Fusion* **60** 066026

[33] Molina Cabrera P A, Kasparek W, Happel T, Eixenberger H, Kammerloher L, Hennequin P and Höfler K 2023 W-band tunable, multi-channel, frequency comb Doppler backscattering diagnostic in the ASDEX-Upgrade tokamak *Rev. Sci. Instrum.* **94** 083504